Seasonal Shifts in Sediment Phosphorus Pools and Their Potential Bioavailability in Aquatic Environments

Gulfam Mohi Ud Din[123*] Ding Fei[123], Nodir Abdushakhidov[123], Usmonov Bakhodirjon Zoir Ugli[4], Maksud Abbaskhanov[5], Satbay Nurjanov[6]

1. School of Water and Environment, Chang'an University, Xi'an 710054, China
2. Key Laboratory of Subsurface Hydrology and Ecological Effect in Arid Region of the Ministry of Education, Chang'an University, Xi'an 710054, China
3. Key Laboratory of Eco-hydrology and Water Security in Arid and Semi-arid Regions of Ministry of Water Resources, Chang'an University, Xi'an 710054, China
4. Faculty of International Educational Programs, Tashkent State Transport University, Tashkent 100167, Uz-bekistan
5. Directorate for the Construction of New Tashkent City" under the Cabinet of Ministers, Tashkent, Uzbekistan
6. Tashkent Institute of Irrigation and Agricultural Mechanization Engineers" National Research University, Tashkent 100000, Uzbekistan

**Corresponding author: Gulfam Mohi Ud Din, e-mail: gulfammohiuddin@gmail.com*

Abstract

Freshwater ecosystems are increasingly threatened by anthropogenic pressures such as urbanization, deforestation, untreated sewage discharge, and waste dumping, which accelerate nutrient enrichment and eutrophication in river systems. This paper examines the dynamics of sediment phosphorus fractions and bioavailability to determine eutrophication potential in different land-use categories and seasons. Mean exchange resin-extractable (bioavailable) P in sediments followed the sequence: anthropogenic > Poultry/Diffuse pollution > outlet > forest fires, > agriculture > waste dumping > forest, with maximum concentrations reaching ~70 mg kg^{-1} during December 2024. Similarly, both labile-P and moderately labile-P fractions were substantially elevated in anthropogenic and waste-impacted locations, indicating enhanced internal phosphorus loading and eutrophication potential. Total phosphorus (TP) was highest at anthropogenic (1521.4 mg kg^{-1}) and waste-dumping sites (1506.1 mg kg^{-1}), whereas forest sites consistently showed the lowest phosphorus accumulation. Seasonal trends revealed increased eutrophication risk during post-monsoon and late dry periods, with the eutrophication index peaking at 0.090 in December 2024. This study integrates sequential sediment phosphorus

ACCEPTED MANUSCRIPT

fractionation with the proposed Sediment Eutrophication Risk Index (SERI) to characterize phosphorus mobility, bioavailability, and sediment-associated eutrophication risk across contrasting land-use and pollution-source settings in a monsoon-influenced Himalayan catchment. The findings demonstrate that anthropogenic activities strongly regulate phosphorus bioavailability and eutrophication risk in the Goi-Nala catchment and provide a transferable framework for nutrient management and eutrophication assessment in monsoon-influenced river systems.

Keywords: Phosphorus; Fractionation; Sediments; Bioavailability; River Jhelum, Catchment; anthropogenic Activities

1. Introduction

Land degradation in river catchments caused by anthropogenic activities has become a major global concern (Gavrilaș et al., 2025). One of the major consequences of such degradation is the increase in sediment loads in rivers, which leads to reservoir sedimentation, eutrophication, and deterioration of water quality (Tundu et al., 2018). The Anthropocene has been suggested a new geologic epoch in which human activities have become a dominant force influencing earth's ecosystems (Zalasiewicz et al., 2011). High anthropogenic pressure, often associated with ecological stress, is typically observed in urban and industrial areas where untreated sewage and municipal effluents are discharged into nearby water bodies (Ferreira et al., 2018).

Agricultural discharge is widely recognized as a major source of nitrogen (N) and phosphorus (P) inputs into riverine systems (Xia et al., 2020). However, the magnitude of nutrient loading varies globally depending on the soil characteristics, agricultural practices, and fertilizer application rates (McDowell et al., 2021). Such variability has been documented in different regions including, Asia (Zhu et al., 2020), Australia and New Zealand (McDowell et al., 2021), Europe (Jarvie et al., 2006), South America (Zafar et al., 2016), and the USA (Sharpley et al., 2013).

In addition to nutrient enrichment, excessive sedimentation poses a serious threat to the sustainability of streams and rivers (Zafar et al., 2016). Soil erosion has become a significant environmental issue in both developed and developing countries. Evidence of historical, ongoing, and accelerating soil erosion has been reported across many regions of the world, particularly in areas with a long history of human activity (Chase et al., 2015). Numerous studies have demonstrated that agricultural and grazing practices significantly influence erosion

ACCEPTED MANUSCRIPT

processes (Centeri, 2022), and in some cases their impacts may even exceed those associated with climate change.

Catchment-scale hydro-morphological studies are effective for evaluating landscape functioning by integrating runoff generation, sediment transport, and biogeochemical cycling (Babur et al., 2020; Chase et al., 2015). River sediments can act as important reservoirs of nutrients and other pollutants and may subsequently contribute to internal nutrient loading and deterioration of water quality (Singh & Rupp, 2026; Sridhar, 2026)). Therefore, spatially and seasonally resolved geochemical assessments are needed to better understand sediment-associated phosphorus dynamics and identify areas vulnerable to eutrophication.

Despite extensive research on phosphorus dynamics, eutrophication in freshwater ecosystems and environmental monitoring (Zhu et al., 2020; Jarvie et al., 2006; Maruthai et al., 2025; Sivasubramanian et al., 2025; Selvanarayanan et al., 2024), phosphorus studies in Pakistan have largely focused on water quality, nutrient enrichment, soils, lakes, reservoirs, and general sediment contamination, while detailed sediment phosphorus fractionation in river catchments remains limited. Similarly, research in the Jhelum basin has mainly addressed sediment yield, water-quality degradation, nutrient enrichment, and contaminant distribution, with limited attention to the seasonal partitioning and bioavailability of sediment phosphorus in tributary catchments such as Goi-Nala. This is important because total phosphorus does not distinguish among pools with different mobility, whereas fractionation alone does not provide an integrated assessment of eutrophication risk. Moreover, conventional eutrophication assessments primarily emphasize water-column nutrient concentrations and trophic status, potentially overlooking the contribution of sediment-bound phosphorus to internal loading.

To address these gaps, this study integrates sequential sediment phosphorus fractionation with bioavailable phosphorus measurements and the proposed Sediment Eutrophication Risk Index (SERI) to evaluate sediment-associated phosphorus mobility and eutrophication risk in the Goi-Nala Catchment. The novelty lies in combining multiple sediment phosphorus pools with bioavailable phosphorus within a single sediment-based risk framework and applying it across contrasting land-use and pollution-source settings under monsoon and dry-period conditions. SERI complements existing phosphorus and eutrophication indices by providing a spatially and seasonally comparable assessment that incorporates sediment phosphorus characteristics and their potential contribution to internal phosphorus loading. In addition, the study examines short-

ACCEPTED MANUSCRIPT

term particulate phosphorus dynamics entering the river to evaluate its potential role as a phosphorus sink or source under contrasting environmental conditions.

2. Materials and methods

2.1 Study site

The study catchment Goi-Nala map is shown in Figure 1. Most part of the catchment is mountainous with steep slopes, hilltops and ridges. The area has been generally covered with open woodland vegetation dominated by pine trees for hundreds of years. Natural forest consists of Sub-tropical pine forests having Chirpine (Pinus roxburghii) forests mixed with some broadleaved species. In moist and dry temperate regions, Bluepine (Pinus wallichina) is the main conifers interspersed with certain broadleaved associates (Maple, Horsechestnut, Birdcherry, Palach, Walnut, etc.). However, changes in vegetation-cover or removal of natural vegetation have resulted in a drastic effect on the soil and water quality. The altitude lies between the 500–1200 m above sea level in the northeast of Pakistan under the foothills of great Himalayas at Poonch division, AJK, Pakistan. The study catchment is characterized by annual rainfall ranging from 500−2000 mm (depending on season), most of which is irregular and falls as intense storms during the monsoon and sometimes in winter. The climate is characterized by hot summers, with maximum temperatures reaching about 38 °C, whereas winters are relatively cold, with temperatures occasionally falling below the freezing point.

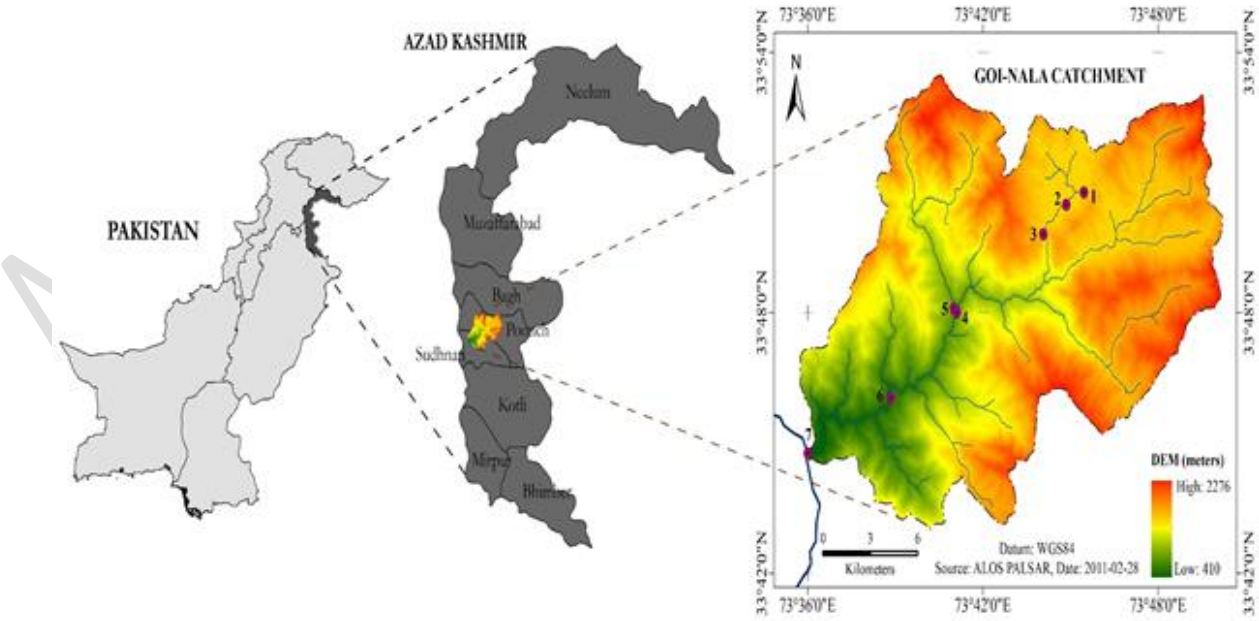


Fig. 1 Location of the Goi-Nala catchment in the River Jhelum basin, Azad Jammu and Kashmir, Pakistan

2.1.1 Selection of representative monitoring stations

Digital elevation models of the catchment were developed using elevation data. Then, sub-catchments were delineated using GIS terrain analysis tools on the basis of elevation, slope and topography. The land use and land cover maps from catchment was generated by Digital Elevation Model (DEM) of 12.5 meters (ALOS PALSAR, source https://www.asf.alaska.edu/) and the drainage network was extracted from the DEM using a flow-accumulation threshold of 11,000. We selected 7 monitoring stations in the month of June 2024 at sub-catchments scale and delineation was carried by using GIS terrain analysis tools on the basis of elevation, slope and topography.

Table 1 Seven monitoring points with their description

Point No.	Station Name and Code	Latitude (N)	Longitude (E)	Altitude (m)	Major Land-Use
1	Forest (L1)	33°50′770″	73°45.459″	1658	Least anthropogenic / Predominant Forest
2	Chal Trar (L2)	33°50′486″	73°44′852″	1584	Highly polluted / After city / Effluent etc.
3	Lower Topa (L3)	33°49′811″	73°44′068″	1510	After city dumping site
4	Du Khadi (L4)	33°48′096″	73°41′006″	884	Mixed land use / Cultivated
5	Bar Sharif (L5)	33°48′002″	73°41′106″	871	Plandri site, forest fires etc.
6	Tamra (L6)	33°46′036″	73°38′828″	619	Poultry Diffuse pollution
7	Azad Pattan (L7)	33°44′756″	73°36′001″	456	Catchment outlet

2.2 Collection and preparation of sediments

Suspended sediment samples were collected from seven monitoring stations using time-integrated suspended sediment samplers following the methodology described by Phillips et al. (2000). The samplers were initially deployed at all monitoring stations in early June 2024, and the first sediment samples were retrieved in July 2024. Following each sampling event, the samplers were redeployed at the respective monitoring stations to ensure continuous collection of suspended sediments throughout the study period. This deployment–retrieval cycle was repeated until the end of the study period in August 2025. In total, six sampling campaigns were conducted in July 2024, September 2024, December 2024, March 2025, June 2025, and August 2025, representing contrasting seasonal conditions. The collected sediment samples were oven-dried at 50 °C and sieved to <63 μm for chemical analyses, while additional material was passed through a 2 mm sieve for particle-size distribution analysis.

2.2.1 Data quality assurance and validation

ACCEPTED MANUSCRIPT

To ensure the reliability and consistency of field and laboratory data, standardized sampling and analytical protocols were followed throughout the study period. Suspended sediment samples were collected using a consistent time-based sampling strategy at all monitoring stations. In the laboratory, all chemical analyses were performed in triplicate (n = 3), and results were reported as mean values with standard errors. Analytical precision was assessed using replicate analyses and procedural blanks during the digestion and extraction procedures. The relative standard deviation (RSD) of replicate measurements was calculated to assess analytical precision. Instrument calibration was performed before each analytical batch following standard laboratory protocols. These quality-control procedures were used to verify the accuracy, precision, and reproducibility of the analytical results.

2.2.2 Phosphorus fractionation

Sediment samples were sieved to 63 μm for all analyses. Phosphorus fractions were determined using the Hedley fractionation scheme proposed by Hedley et al. (1982) with slight modifications by Condron Condron et al. (1985), and subsequent applications to fluvial sediments (Li et al., 2022). For each analysis, 0.5 g of the <63-μm sediment fraction was used. For each extraction step, 10 mL of the respective extracting solution was added to the sediment sample, and the suspension was mixed using an end-over-end shaker for 24 h. Following each extraction step, the extract was separated from the sediment residue according to the procedure shown in Figure 2, and the residue was subsequently subjected to the next extraction step. Total phosphorus (TP) was determined separately after digestion of 0.5 g of sediment using H_2SO_4 and H_2O_2 in the presence of saturated $MgCl_2$. Phosphorus concentrations in the resulting extracts and digests were determined colorimetrically following the Murphy & Riley (1962) method.

ACCEPTED MANUSCRIPT

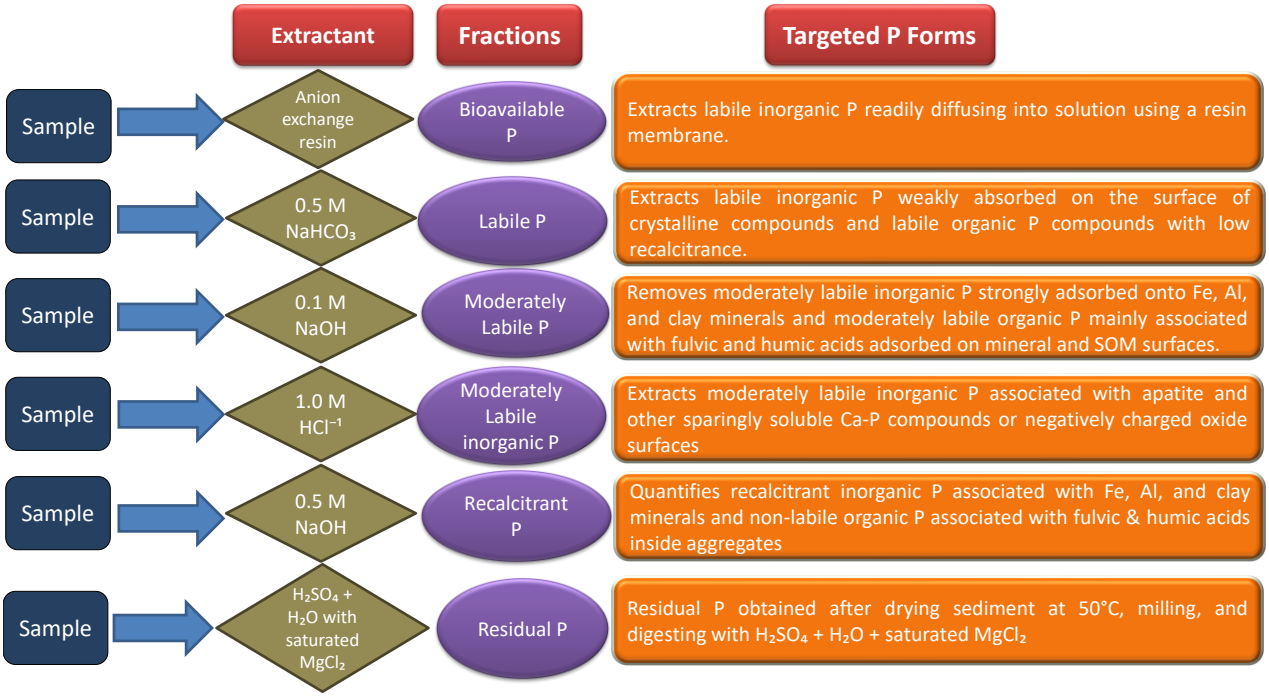


Fig. 2 Flow diagram of modified Hedley et al. (1982) P fractionation scheme

The selected phosphorus fractions were chosen because they represent the principal geochemical phosphorus pools that differ in mobility, chemical stability, and bioavailability (Condron et al., 1985; Li et al., 2022). Bioavailable phosphorus represents the fraction immediately available for algal uptake, whereas $NaHCO_3$-extractable, NaOH-extractable, HCl-extractable, and residual phosphorus represent labile, moderately labile, mineral-bound, and stable phosphorus pools, respectively. Collectively, these fractions provide a comprehensive characterization of sediment phosphorus dynamics and their potential contribution to internal phosphorus loading and eutrophication risk, thereby forming the basis for the proposed Sediment Eutrophication Risk Index (SERI).

2.2.3 Complementary physicochemical analysis of catchment soils

Total organic carbon (TOC) was determined using the modified Mebius method (Nelson & Sommers, 1983). 0.5 g of soil samples were taken in digestion tubes with 4 mL of H_2SO_4, ¼ of a digestion tablet in each tube, and digested at 150 °C for 30 min. The digests were then titrated with a standardized $FeSO_4$ solution. Soil-bound total nitrogen (TN) was determined by the Kjeldahl digestion method (Bremner et al., 2018). Similarly, the per cent particle size distribution (sand, silt, and clay) was determined using the Bouyoucos hydrometer method (Bouyoucos, 1962).

2.3 Sediment Eutrophication Risk Index (SERI)

To evaluate the eutrophication potential of sediments in the Goi-Nala Catchment, Sediment based Eutrophication Risk Index (SERI**)** was developed by integrating sediment phosphorus fractionation and bioavailability data. The index quantifies the relative risk of internal phosphorus loading from sediments to the overlying water column. SERI was calculated using the following expression:

$$SERI = \frac{(L-P+M-P)}{T-P} \times \frac{BAP}{Max(BAP)} \qquad (1)$$

Note, L-P represents the labile phosphorus fraction (including exchangeable-P and Fe/Al-bound P), M-P denotes the moderately labile phosphorus fraction (e.g., Ca-bound P), T-P is the total phosphorus content of the sediment, and BAP refers to bioavailable phosphorus determined by the exchange resin extraction method. The Max (BAP) term corresponds to the highest BAP value observed across all samples and serves as a normalization factor to scale the index between 0 and 1.

The variables were selected based on their theoretical relevance to sediment phosphorus mobility and bioavailability. L-P and M-P represent potentially mobile phosphorus pools, while T-P represents the total sediment phosphorus reservoir. BAP was included to account for the relative biologically available phosphorus pool. The weighting scheme is theoretical rather than empirically calibrated; no independent dataset or optimization procedure was used to assign differential weights. L-P and M-P were therefore given equal contribution through their additive combination, while BAP was normalized using Max (BAP).

SERI is intended as a relative screening indicator of sediment eutrophication potential. Uncertainty may arise from analytical variability, phosphorus fraction classification, BAP measurements, and the normalization procedure. The lack of independent calibration and formal sensitivity analysis is therefore recognized as a limitation, and future studies should validate SERI using independent datasets and controlled phosphorus-release experiments.

2.4 Statistical Analysis

Statistical analyses were performed using SPSS (version 11.2). Because the dataset did not meet normality assumptions, the non-parametric Kruskal–Wallis test was applied to evaluate significant differences among sampling locations and seasons. Each measurement was conducted in triplicate (n = 3), and results are presented as mean ± standard error. When significant

ACCEPTED MANUSCRIPT

differences were detected ($p < 0.05$), pairwise comparisons among groups were examined to identify the relative differences between locations and seasons. Additional statistical visualization and mapping analyses were performed using Statistix 8.1, SigmaPlot 12.0, and Python. All datasets analyzed in this study were generated from field-collected sediment samples and laboratory measurements conducted specifically for the present investigation.

3. Results

3.1 Basic properties of catchment soils

The basic physicochemical properties of catchment topsoil collected from 13 sampling locations are presented in Table 2. The sampling sites represented three major land-use types: forest land, grassland, and arable land. Overall, the contents of total organic carbon (TOC), total nitrogen (TN), available phosphorus (AP), and available potassium (AK) followed the general trend: forest > grassland > arable land.

Soil samples collected from different elevations across the catchment (~700–1,970 m) exhibited considerable spatial variability in their physicochemical characteristics. Soil texture ranged from sandy loam to silty clay, with sand, silt, and clay contents varying between 16–56%, 27–55%, and 16–34%, respectively. Electrical conductivity (EC) values were relatively low (0.6–1.8 dS m^{-1}), indicating non-saline soil conditions, while soil pH ranged from slightly acidic to moderately alkaline (6.8–7.9).

Organic matter (OM) content ranged from 5–39 mg kg^{-1}, whereas total nitrogen (TN) varied between 0.05 and 1.8 mg kg^{-1} across the sampling locations. Available phosphorus (AP) concentrations ranged from 4 to >17 mg kg^{-1}, reflecting differences associated with land use and site management practices. Statistical analysis showed that EC, OM, TN, and AP had coefficients of variation (CV) greater than 25%, indicating substantial spatial heterogeneity within the Goi-Nala catchment soils.

Table 2 Basic soil physicochemical properties of the top soil (0-15 cm) at 13 selected sites (each has Forest, Grassland and Arable) in Goi-Nala catchment

Nfg	Latitude N	Longitude E	Point Name	Height (m)	% Sand	% Silt	% Clay	pH	EC (dS/m)	OM ($mgkg^{-1}$)	TN ($mgkg^{-1}$)	AP ($mgkg^{-1}$)
F0	33°50′ 52.44″ N	73°42′ 53.11″ E	Upper topa	1968	50.54	31.4	18.16	7.2	1.38	28.8	1.01	6.44
F1	33°50′ 52.44″ N	73°46′ 52.82″ E	Chak	1698	48.42	33.4	16.16	7.48	1.07	38.8	1.37	12.24

ACCEPTED MANUSCRIPT

G1	33°51′ 10.17″ N	73°47′ 01.89″ E	Chak	1694	32.44	39.4	28.16	7.31	0.92	27.4	0.59	10.23
A1	33°50′ 57.88″ N	73°46′ 59.2″ E	Chak	1652	44.44	35.4	20.16	7.47	1.19	12.56	0.063	6.44
F2	33°51′ 11.93″ N	73°43′ 52.1″ E	Kharic	1630	24.44	45.4	30.16	6.98	0.86	21.4	0.79	17.34
G2	33°51′ 08.82″ N	73°43′ 46.93″ E	Kharic	1628	34.44	41.4	24.16	7.12	1.25	17.1	0.66	5.24
A2	33°51′ 08.96″ N	73°44′ 14.63″ E	Kharic	1618	40.44	36	23.56	7.4	1.06	16.05	0.72	6.33
F3	33°52′ 07.51″ N	73°44′ 57.17″ E	Pothi	1698	41.84	31.4	26.76	7.53	1.36	17.1	0.92	7.44
G3	33°52′ 07.11″ N	73°44′ 54.9″ E	Pothi	1710	32.44	42.8	24.76	7.79	0.71	16.2	0.9	6.46
A3	33°51′ 51.01″ N	73°44′ 55.87″ E	Pothi	1672	20.44	55.4	24.16	7.24	0.75	8.8	0.46	3.94
F4	33°48′ 49.79″ N	73°45′ 35.1″ E	Dareek	1773	24.44	51.4	24.16	7.15	1.23	27.92	1.78	11.64
G4	33°48′ 48.53″ N	73°45′ 50.96″ E	Dareek	1771	16.44	55.4	28.16	7.78	1.56	25.6	1.36	14.45
A4	33°48′ 54.67″ N	73°45′ 33.83″ E	Dareek	1766	50.44	27.44	22.16	7.75	0.93	13.26	0.66	8.25
F5	33°48′ 43.03″ N	73°43′ 21.96″ E	Maidan	1414	29.84	49.4	20.76	7.74	0.59	18.2	0.92	4.56
G5	33°48′ 46.32″ N	73°43′ 22.41″ E	Maidan	1453	22.44	43.4	34.16	7.78	1.6	7.4	0.84	5.58
A5	33°48′ 45.04″ N	73°43′ 27.51″ E	Maidan	1427	32.44	43.4	24.16	7.29	0.68	6.6	0.38	9.78
F6	33°49′ 42.35″ N	73°41′ 05.96″ E	Khad	1526	56.44	23.4	20.16	6.84	1.05	14.92	0.75	12.44
G6	33°49′ 36.85″ N	73°41′ 13.87″ E	Khad	1522	19.84	54	26.16	7.02	1.15	12.9	1.25	7.95
A6	33°49′ 41.32″ N	73°41′ 11.66″ E	Khad	1530	46.44	38	15.56	7.24	1.18	18.5	0.92	6.35
F7	33°49′ 54.6″ N	73°39′ 21.2″ E	Chiraan	1409	28.14	43.7	28.15	7.58	0.78	15.5	1.19	13.44
G7	33°49′ 52.8″ N	73°39′ 30.29″ E	Chiraan	1371	32.44	42.8	24.76	7.32	0.84	12.2	1.32	12.42
A7	33°49′ 59.34″ N	73°39′ 24.29″ E	Chiraan	1363	20.44	55.4	24.16	7.56	1.25	15.2	0.67	6.46

ACCEPTED MANUSCRIPT

F8	33°47′ 07.37″ N	73°41′ 33.74″ E	Dewan Gura	1184	2044	55.4	24.16	7.34	1.33	15.6	0.72	7.44
G8	33°47′ 03.95″ N	73°41′ 35.82″ E	Dewan Gura	1192	16.44	55.4	28.16	7.36	1.05	15.8	0.86	8.56
A8	33°47′ 08.08″ N	73°41′ 37.25″ E	Dewan Gura	1217	50.44	27.4	22.16	7.52	1.56	15.4	0.46	7.78
F9	33°47′ 57.53″ N	73°39′ 17.51″ E	Chattar Kot	1196	29.84	49.4	20.76	7.22	1.45	11.2	0.78	6.36
G9	33°47′ 54.94″ N	73°39′ 15.76″ E	Chattar Kot	1166	32.44	43.4	24.16	7.24	1.23	9.8	0.76	5.83
A9	33°47′ 58.31″ N	73°39′ 14.16″ E	Chattar Kot	1188	24.44	51.4	24.16	7.56	1.44	9.4	0.73	14.24
F10	33°47′ 55.72″ N	73°40′ 41.29″ E	Challar	1043	56.44	23.4	20.16	7.24	1.26	15.4	1.22	8.24
G10	33°47′ 53.39″ N	73°40′ 39.94″ E	Challar	1032	22.44	43.4	34.16	7.44	1.18	7.8	0.56	4.22
A10	33°47′ 51.16″ N	73°40′ 42.95″ E	Challar	1027	24.44	51.4	24.16	7.36	1.44	8.8	0.52	6.35
F11	33°45′ 05.16″ N	73°40′ 24.57″ E	Nab	1450	16.44	55.4	28.16	7.84	1.78	9.6	1.06	5.56
G11	33°45′ 67.41″ N	73°40′ 39.87″ E	Nab	1371	50.44	27.4	22.16	7.76	1.22	6.4	0.65	8.49
A11	33°45′ 08.77″ N	73°40′ 23.39″ E	Nab	1427	29.84	49.4	20.75	7.88	1.56	7.6	0.44	6.87
F12	33°45′ 07.33″ N	73°38′ 09.91″ E	Sawan	856	22.44	43.4	34.16	7.8	1.78	14.4	0.92	5.44
G12	33°45′ 07.07″ N	73°38′ 15.42″ E	Sawan	852	32.44	43.4	24.16	7.44	1.56	12.4	0.78	6.66
A12	33°45′ 06.84″ N	73°38′ 13.84″ E	Sawan	860	32.44	43.4	24.16	7.56	1.58	6.6	0.26	4.23
F13	33°45′ 46.54″ N	73°37′ 55.12″ E	Pattan	701	20.44	55.4	24.16	7.88	1.66	8.8	0.62	7.89
G13	33°45′ 43.96″ N	73°37′ 55″ E	Pattan	687	24.44	51.4	24.16	7.72	1.24	5.6	0.33	5.43
A13	33°45′ 41.88″ N	73°37′ 53.28″ E	Pattan	668	46.44	31.4	22.16	7.83	1.77	5.8	0.44	5.66
Minimum					8.02	36.41	5.40	6.84	0.59	1.52	0.05	3.94
Maximum					51.98	81.47	19.74	7.88	1.78	6.26	0.33	17.34
SD					3.01	10.45	10.75	0.27	0.31	1.14	0.06	3.20
CV					30.88	18.88	30.47	3.64	25.84	57.37	35.50	39.94

ACCEPTED MANUSCRIPT

3.2 Algal bioavailable-P content under different land-use/pollution sources

As shown in Figure 3, sediment anion exchange resin extractable phosphorus (algal bioavailable P) exhibited statistically significant differences ($p < 0.05$) across locations. Pairwise comparisons indicated that anthropogenic and Poultry/Diffuse pollution locations showed significantly higher bioavailable P concentrations compared with forest and outlet sites. anthropogenic sites exhibited the highest bioavailable P concentrations (51.97 mg kg^{-1}), whereas forest locations showed the lowest values (4.46 mg kg^{-1}). Intermediate concentrations were observed at Poultry/Diffuse pollution, outlet, forest fires, agriculture, and waste dumping sites. Considering temporal variation, bioavailable P concentration showed clear spatial differences across both monitoring years. The highest concentrations were consistently observed at locations 2 and 3, particularly during December 2024, whereas location 1 maintained the lowest values throughout the study period. A similar distribution pattern was observed during 2025, indicating persistent phosphorus enrichment at anthropogenic and impacted locations. Elevated bioavailable P concentrations at these sites likely reflect increased nutrient inputs associated with human activities and surface runoff processes.

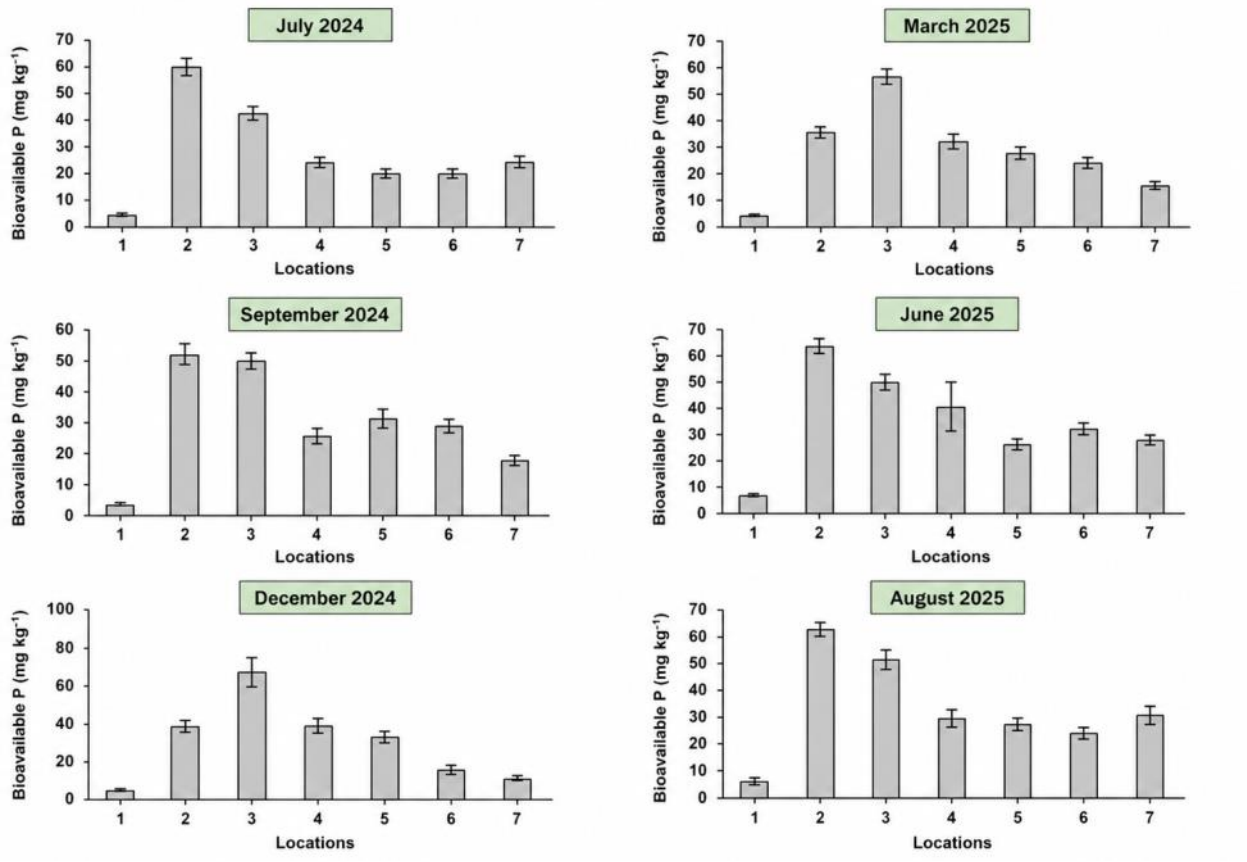


Fig. 3 Temporal variations in sediment anion exchange resin membrane-extractable phosphorus (algal bioavailable-P) content (mg kg^{-1}) at seven sampling locations (L1–L7) during 2024 and 2025. Error bars indicate mean ± standard error (n = 3).

3.3 0.5 M $NaHCO_3$–P_t under different land-use/pollution sources

As shown in Figure 4, sodium bicarbonate extractable total phosphorus (0.5 M $NaHCO_3$–P_t) displayed significant spatial variability across locations. Outlet and anthropogenic sites recorded the highest concentrations (128.7 and 119.3 mg kg^{-1}, respectively), whereas forest and agricultural locations showed comparatively lower values (30.4 and 38.9 mg kg^{-1}, respectively). Intermediate concentrations were observed at forest fires, Poultry/Diffuse pollution, and waste dumping sites. Temporal variation indicated that elevated $NaHCO_3$–P_t concentrations were consistently associated with outlet and anthropogenic locations during both 2024 and 2025, with relatively higher values observed during December 2024. In contrast, forest and agricultural sites maintained lower phosphorus concentrations throughout the study period. These findings suggest persistent phosphorus accumulation at outlet and anthropogenic locations, likely due to enhanced nutrient transport, anthropogenic inputs, and downstream sediment deposition processes.

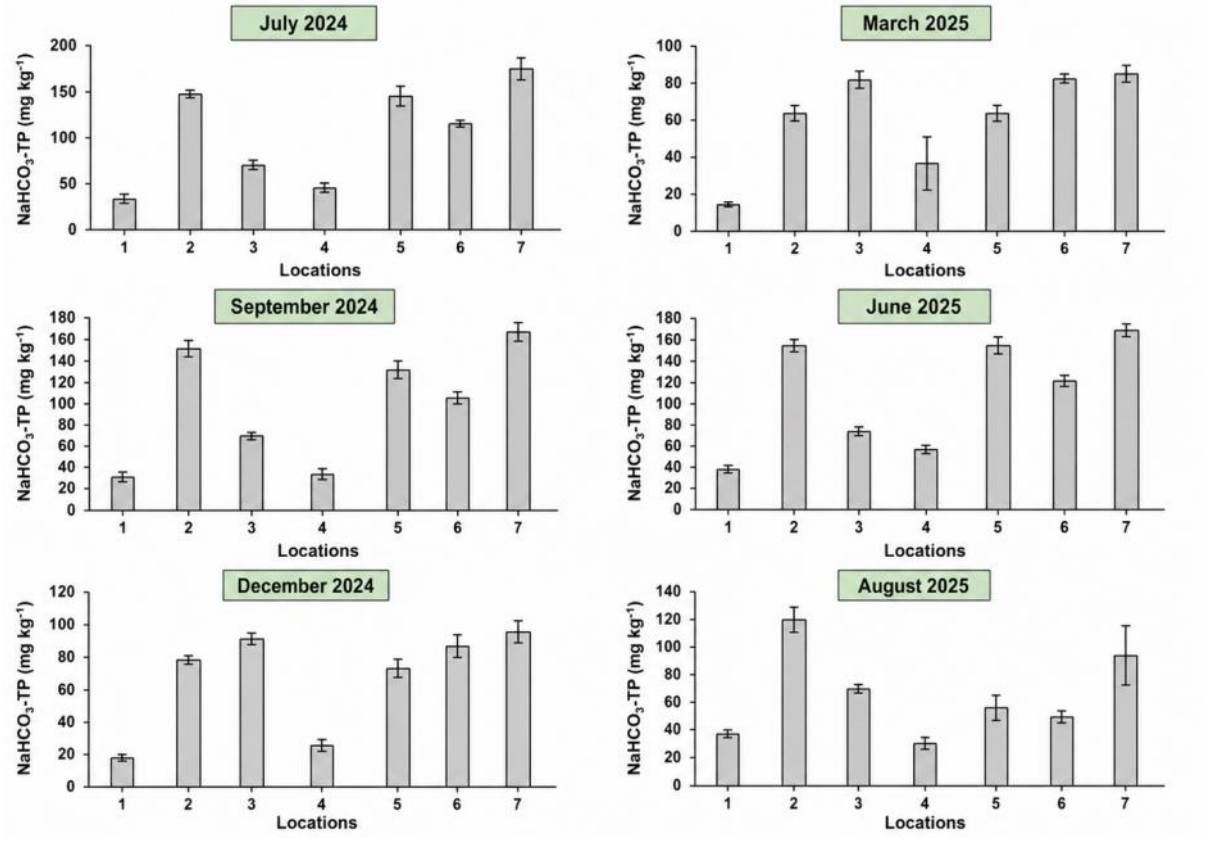


Fig. 4 Temporal variations in sediment sodium bicarbonate-extractable total phosphorus ($NaHCO_3$–TP) content (mg kg^{-1}) at seven sampling locations (L1–L7) during 2024 and 2025 Error bars represent mean ± standard error (n = 3).

3.4 0.1 molar sodium hydroxide extractable phosphorus fractions

Sediment 0.1 M sodium hydroxide-extractable total phosphorus (0.1 M NaOH–Pt) showed significant spatial and seasonal variations ($p < 0.05$), as shown in Figure 5. Pairwise comparisons indicated that waste dumping and anthropogenic sites contained significantly higher phosphorus concentrations than forest and outlet locations. The highest mean 0.1 M NaOH–Pt concentrations were recorded at waste dumping (271.7 mg kg^{-1}) and anthropogenic sites (270.8 mg kg^{-1}), whereas comparatively lower values were observed at outlet and forest locations. Intermediate concentrations occurred at agricultural and Poultry/Diffuse pollution sites.

Overall, elevated NaOH-extractable phosphorus fractions at anthropogenic and waste dumping location indicate enhanced accumulation of Fe/Al-associated phosphorus in sediments influenced by human activities and nutrient enrichment processes.

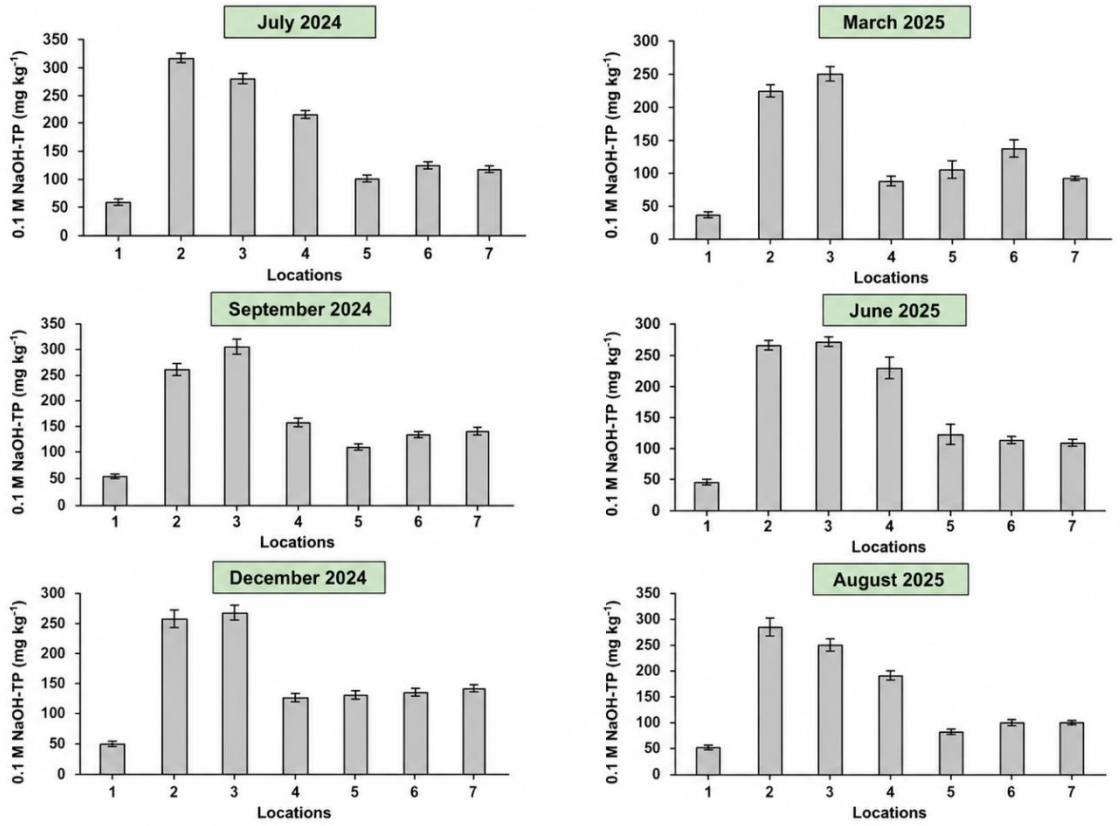


Fig. 5 Temporal variations in sediment 0.1 M sodium hydroxide-extractable total phosphorus (0.1 M NaOH–TP) content (mg kg^{-1}) at seven sampling locations (L1–L7) during 2024 and 2025 Error bars represent mean ± standard error (n = 3).

3.5 Inorganic P (mg kg^{-1}) under different land-use types/pollution sources

Sediment 1.0 M hydrochloric acid-extractable phosphorus showed significant spatial and seasonal variations ($p < 0.05$), as illustrated in Figure 6. Pairwise comparisons indicated that waste dumping and anthropogenic locations had significantly higher phosphorus concentrations than forest and outlet sites, reflecting stronger phosphorus accumulation in human-impacted areas.

Waste dumping and anthropogenic sites recorded the highest mean HCl-extractable phosphorus concentrations (387.1 and 384.3 mg kg^{-1}, respectively), whereas forest and outlet locations showed comparatively lower values (151.8 and 201.1 mg kg^{-1}, respectively). Intermediate concentrations were observed at forest fires, agricultural, and Poultry/Diffuse pollution sites. Seasonal variation indicated relatively higher inorganic P concentrations during July and September 2024, while comparatively lower values were recorded during March and June 2025.

Higher HCl-bound phosphorus concentrations may indicate greater accumulation of calcium-associated phosphorus in sediments affected by anthropogenic activities and nutrient loading.

ACCEPTED MANUSCRIPT

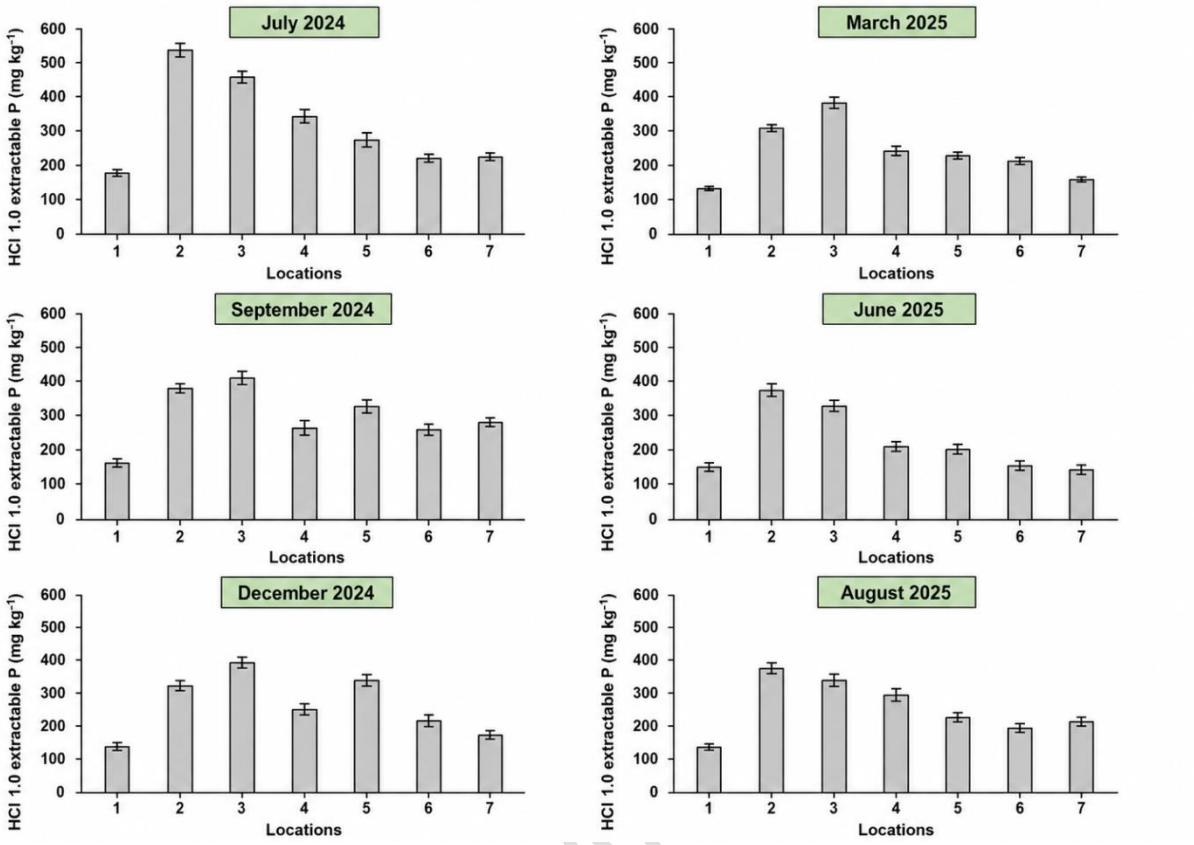


Fig. 6 Temporal variations in sediment hydrochloric acid-extractable phosphorus (HCl-extractable P) content (mg kg^{-1}) at seven sampling locations (L1–L7) during 2024 and 2025 Error bars represent mean ± standard error (n = 3).

3.6 0.5 molar sodium hydroxide extractable phosphorus fractions

Sediment 0.5 M sodium hydroxide-extractable total phosphorus (0.5 M NaOH–Pt) showed significant spatial and seasonal variations ($p < 0.05$), as illustrated in Figure 7. Pairwise comparisons indicated that waste dumping and anthropogenic sites had significantly higher phosphorus concentrations than forest and outlet locations.

The highest mean 0.5 M NaOH–Pt concentrations were recorded at waste dumping (311.5 mg kg^{-1}) and anthropogenic sites (290.6 mg kg^{-1}), whereas lower concentrations were observed at forest and outlet locations (117.9 and 110.8 mg kg^{-1}, respectively). Intermediate values were observed at agricultural, forest fires, and Poultry/Diffuse pollution sites. Seasonal variation showed relatively higher concentrations during September and July 2024, while comparatively lower values were observed during August 2025.

ACCEPTED M

Overall, elevated 0.5 M NaOH–Pt concentrations at anthropogenic and waste dumping sites suggest enhanced phosphorus retention and accumulation in sediments influenced by anthropogenic nutrient inputs and organic matter enrichment.

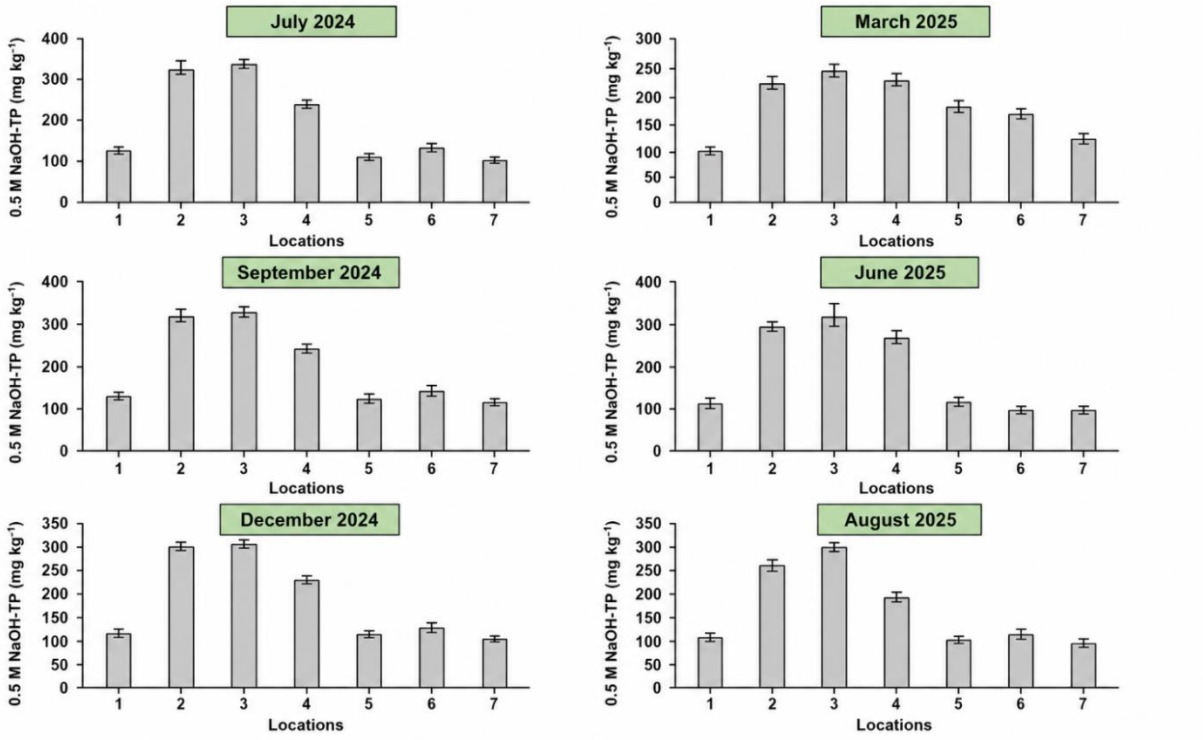


Fig. 7 Temporal variations in sediment 0.5 M sodium hydroxide-extractable total phosphorus (0.5 M NaOH–TP) content (mg kg⁻¹) at seven sampling locations (L1–L7) during 2024 and 2025 Error bars represent mean ± standard error (n = 3).

3.7 Residual Phosphorus content under different land-use types/pollution sources

Sediment residual phosphorus showed significant spatial and seasonal variations ($p < 0.05$), as shown in Figure 8. Pairwise comparisons indicated that anthropogenic and waste dumping locations differed significantly from forest sites, reflecting greater phosphorus accumulation in human-impacted areas. anthropogenic and waste dumping sites recorded the highest mean residual P concentrations (404.4 and 403.78 mg kg⁻¹, respectively), whereas forest and outlet locations exhibited comparatively lower values (190.5 and 219.2 mg kg⁻¹, respectively). Intermediate concentrations were observed at agricultural, forest fires, and Poultry/Diffuse pollution sites. Seasonal variation indicated relatively higher residual P concentrations during July and September 2024, while comparatively lower values were recorded during December 2024 and March 2025. Overall, residual phosphorus represented a

major stable phosphorus pool within the sediments, particularly at anthropogenic and waste dumping locations, suggesting long-term phosphorus accumulation associated with land-use disturbance and nutrient enrichment.

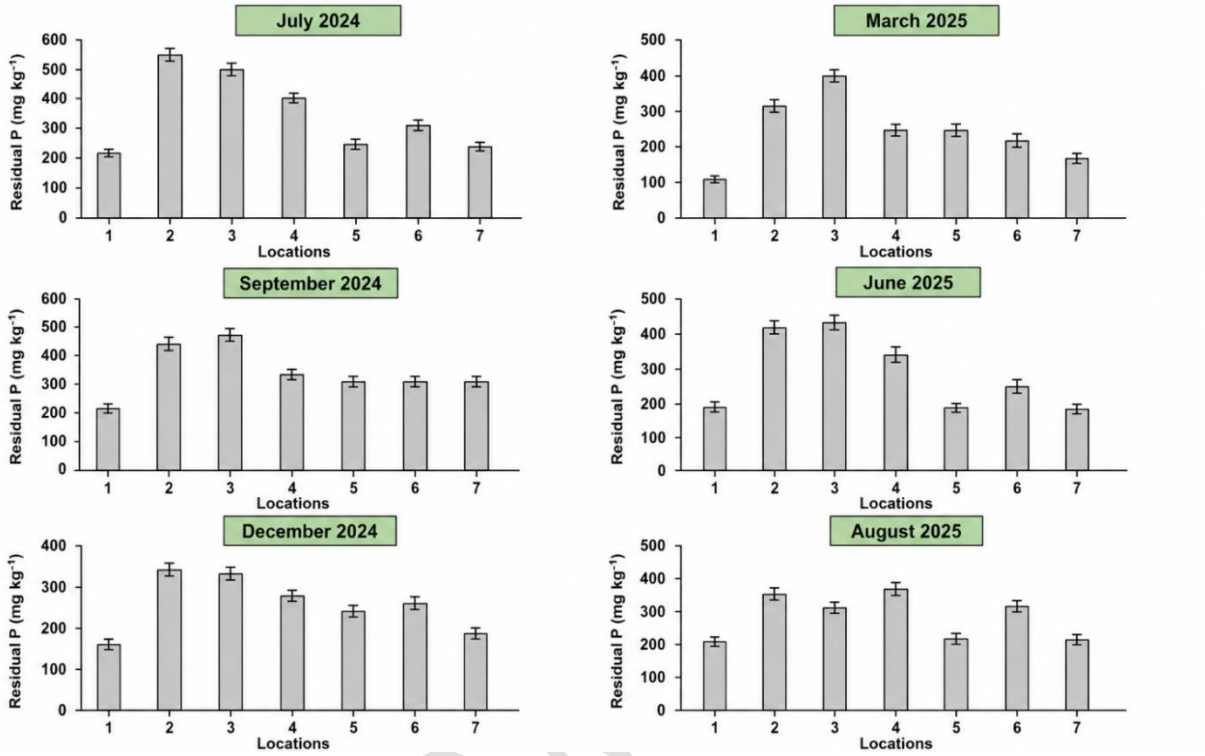


Fig. 8 Seasonal variation in sediment residual phosphorus (Residual-P) concentrations at seven sampling locations (L1–L7) during July 2024–August 2025 Error bars represent mean ± standard error (n = 3). Higher residual phosphorus concentrations at anthropogenic and waste-dumping sites indicate long-term phosphorus accumulation associated with human activities.

3.8 Total P content under different land-use types/pollution sources

Sediment total phosphorus (TP) showed significant spatial and seasonal variations ($p < 0.05$), as presented in Figure 9. Pairwise comparisons revealed that anthropogenic and waste dumping sites had significantly higher total phosphorus concentrations than forest and outlet locations, indicating substantial phosphorus enrichment in human-impacted areas. The highest mean TP concentrations were observed at anthropogenic (1521.4 mg kg^{-1}) and waste dumping sites (1506.1 mg kg^{-1}), whereas comparatively lower values were recorded at forest (547.3 mg kg^{-1}) and outlet (801.2 mg kg^{-1}) locations. Intermediate concentrations occurred at agricultural, forest fires, and Poultry/Diffuse pollution sites. Seasonal variation indicated relatively higher TP concentrations during July and September 2024, while comparatively lower values were

observed during March and August 2025. Overall, anthropogenic and waste dumping locations consistently exhibited elevated TP concentrations, suggesting enhanced phosphorus accumulation associated with land-use disturbance, nutrient loading, and sediment deposition processes.

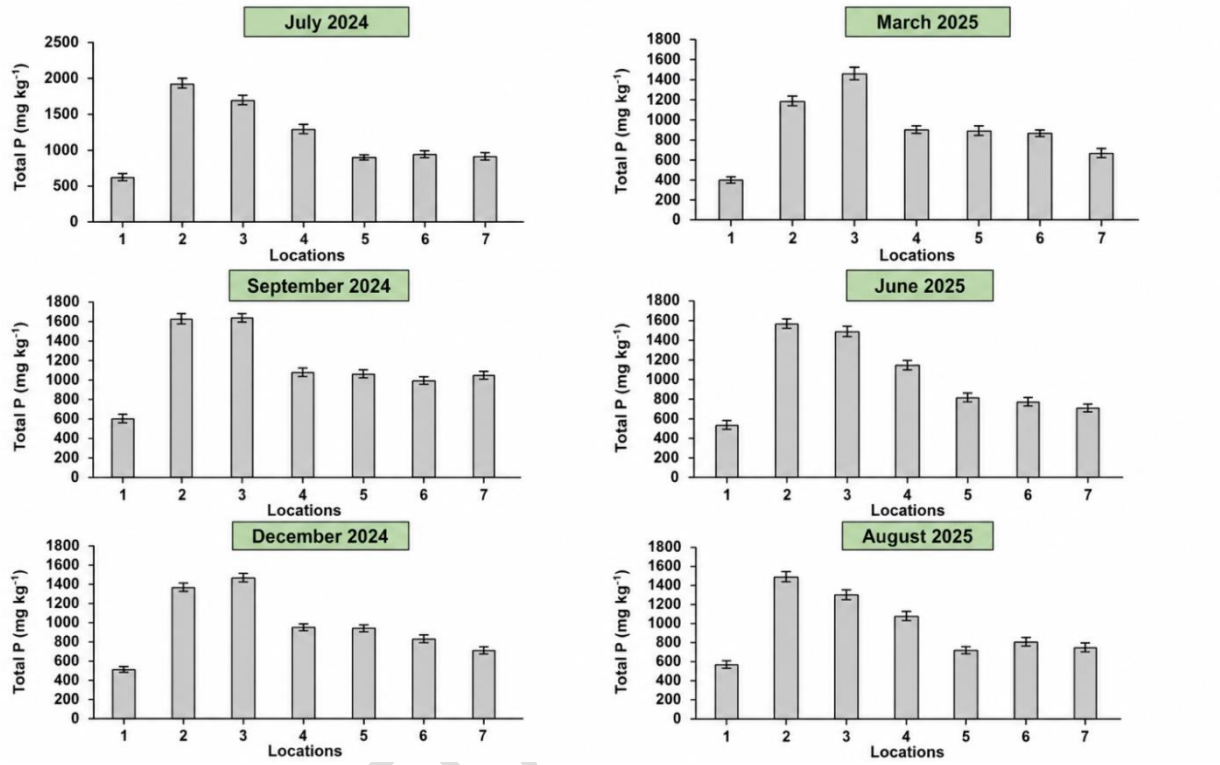


Fig. 9 Seasonal variation in sediment total phosphorus (TP) concentrations at seven sampling locations (L1–L7) during July 2024–August 2025 Error bars represent mean ± standard error (n = 3). Elevated TP concentrations at anthropogenic and waste-dumping sites indicate enhanced phosphorus enrichment resulting from land-use disturbance and sediment deposition.

3.9. Sediment Eutrophication Risk Index

Figure 10 illustrates the seasonal variation of the sediment eutrophication risk index (SERI) across seven monitoring locations (L1–L7) from July 2024 to August 2025. Clear spatial and temporal variations in SERI were observed throughout the study period. Overall, SERI values remained relatively low during the initial monitoring period, with values ranging from 0.005 to 0.010 during July 2024. A moderate increase was observed during September 2024, particularly at the anthropogenic (L2) and waste-dumping (L3) sites, whereas the highest SERI value was recorded during December 2024 at the anthropogenic site (L2; 0.090), indicating elevated eutrophication risk at this location.

ACCEPTED

During 2025, SERI values generally remained moderate, with slight increases observed at several locations during June and August 2025. Among all monitoring sites, L2 consistently exhibited the highest SERI values throughout most seasons, whereas comparatively lower values were observed at the remaining locations. Seasonal trends indicated relatively greater eutrophication potential during post-monsoon and late dry-season periods.

Overall, the elevated SERI values at the anthropogenic site (L2) suggest increased nutrient enrichment and greater susceptibility to sediment-associated eutrophication. This pattern is likely related to enhance nutrient inputs from urban activities, surface runoff, and wastewater-related sources.

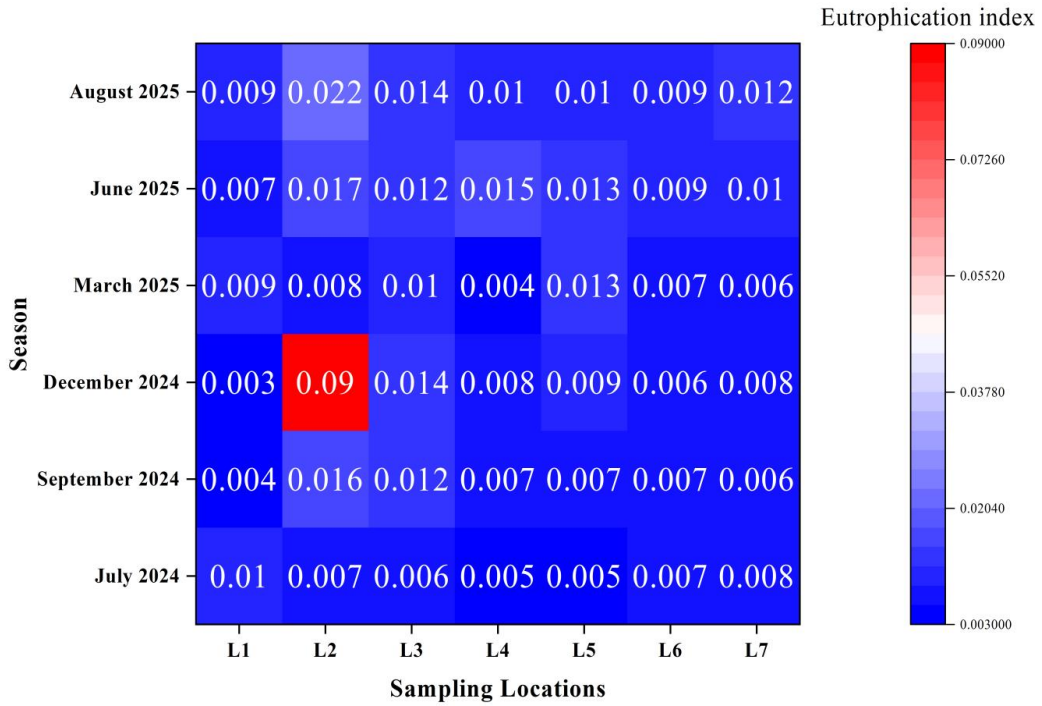


Fig. 10 Seasonal variation of the Sediment Eutrophication Risk Index (SERI) across seven sampling locations (L1–L7) during July 2024–August 2025 Higher SERI values identify locations with greater sediment-associated eutrophication risk, reflecting increased internal phosphorus loading under anthropogenic influence and seasonal hydrological variability.

4. Discussion

4.1 Overall Physicochemical Properties of Soil

The spatial variability observed in soil physicochemical properties across the catchment reflects the influence of land use, vegetation cover, and topographic conditions on soil nutrient dynamics. In the present study, forest soils exhibited comparatively higher TOC, TN, AP, and

AK contents than grassland and arable land soils, likely due to greater organic matter accumulation, litter deposition, and reduced anthropogenic disturbance under forest vegetation cover.

Variations in soil texture were also evident across the catchment, with soils ranging from sandy loam to silty clay. These findings are consistent with previous studies reporting that land-use conversion from forest to cultivated land can alter soil particle distribution and enhance the loss of finer particles through erosion and surface runoff (Lizaga et al., 2019). Forest soils generally retain higher clay and organic matter contents because stable vegetation cover reduces soil disturbance and protects against erosive processes, whereas cultivated and exposed lands are more susceptible to nutrient depletion and topsoil degradation (Nweke et al., 2025).

The relatively high coefficients of variation (CV > 25%) for EC, OM, TN, and AP further indicate substantial spatial heterogeneity within the Goi-Nala catchment. Such variability is commonly associated with differences in land management practices, hydrological pathways, erosion intensity, and nutrient transport processes across watershed systems. Overall, these findings demonstrate that land-use characteristics strongly influence soil physicochemical conditions and nutrient distribution within the Goi-Nala catchment.

4.2 Overall temporal changes in different fractions of P

The elevated concentrations of bioavailable phosphorus observed at anthropogenic and impacted locations in the present study indicate enhanced phosphorus enrichment associated with human activities and surface runoff processes. In contrast, forest locations consistently exhibited the lowest bioavailable P concentrations, suggesting reduced nutrient disturbance and stronger phosphorus retention under stable vegetation cover. The pronounced spatial variability in bioavailable P across the catchment highlights the important influence of land use on sediment phosphorus dynamics. The results for bioavailable phosphorus (P) obtained in this study are consistent with those reported by Vermeiren et al. (2022), who demonstrated that organic residues enhance labile P pools. Similar findings have been reported by Ahmad et al. (2017), indicating that forest cover and organic matter mineralization enhance phosphorus (P) availability in topsoil. Previous studies have also demonstrated that proportion of bioavailable P varies across catchments with different land-use types. For instance, bioavailable P in streams draining forested, mixed-use, and agricultural catchments accounted for 17%, 26%, and 24%,

ACCEPTED MANUSCRIPT

respectively, whereas bioavailable particulate P (%BAPP) in urban sediments averaged 73% during summer but decreased to approximately 19% during storm events (Ellison & Brett, 2006).

The elevated 0.5 M $NaHCO_3$–Pt concentrations observed at outlet and anthropogenic locations in the present study indicates enhanced accumulation and transport of labile phosphorus within the catchment. In contrast, forest and agricultural sites maintained comparatively lower phosphorus concentrations throughout the monitoring period, suggesting reduced nutrient loading and sediment-associated phosphorus deposition in less disturbed areas. Similar trend was reported by Pu et al. (2020) who demonstrated that fluctuations in hydrological conditions significantly influence bioavailable phosphorus concentrations in sediments and increase the potential risk of eutrophication. Increased runoff and sediment transport during wetter periods may enhance the mobilization and downstream accumulation of phosphorus-rich particulates, particularly at outlet and anthropogenic locations. phosphorus Similarly, comparable trends have also been reported by McDowell et al. (2020), who observed that phosphorus enrichment in stream systems promotes algal growth and deteriorates water quality under low-flow and sediment accumulation conditions. Their study further showed that bioavailable phosphorus concentrations tend to increase downstream and accumulate within shallow surface sediments. The elevated $NaHCO_3$–Pt concentrations recorded at outlet sites in the present study therefore likely reflect the cumulative effects of upstream nutrient transport, sediment deposition, and anthropogenic phosphorus inputs.

Organic P was also identified as a significant component of sediment phosphorus pools. Previous studies reported that organic P can account for 21–60% of total P, while bioavailable Po represented 9–34% of organic P (Kianpoor Kalkhajeh, 2019). The main forms of bioavailable Po included labile (H_2O-Po) and moderately labile (NaOH-Po) fractions. Within H_2O-Po, which constituted only 1.4% of Po, about 53% was labile monoester P, 28% was diester P, and 17% was phytate-like P (Babur et al., 2020). These findings highlight the importance of phosphorus fractionation studies in understanding phosphorus mobility and its role in freshwater eutrophication.

Seasonal variations also play a critical role in sediment P mobility. Higher phosphorus (P) release rates have been observed during summer months, while continuous external phosphorus inputs can maintain eutrophic conditions in aquatic systems. Among different

ACCEPTED MANUSCRIPT

phosphorus pools, $NaHCO_3$-extracted and labile fractions have been identified as major contributors to phosphorus release into overlying water (Lv et al., 2024).

The seasonal variations observed in sediment phosphorus fractions are likely influenced by hydrological processes within the catchment. During the monsoon season, increased runoff and soil erosion transport phosphorus-rich particles from agricultural and disturbed lands into the river system, leading to elevated sediment phosphorus concentrations. In contrast, during low-flow periods, reduced water movement promotes sediment deposition and facilitates microbial mineralization and adsorption–desorption processes that regulate the transformation among phosphorus fractions. These mechanisms highlight the strong coupling between hydrological variability and phosphorus cycling within the watershed.

The elevated concentrations of moderately labile phosphorus (0.1 M NaOH–Pt) observed at anthropogenic and waste dumping sites in the present study indicate enhanced accumulation of Fe/Al-associated phosphorus in sediments influenced by human activities and nutrient enrichment processes. In contrast, lower concentrations at forest and outlet locations suggest comparatively lower phosphorus loading and reduced sediment contamination under less disturbed environmental conditions. These findings are consistent with previous studies reporting that organic residues, vegetation cover, and nutrient cycling processes can enhance moderately labile phosphorus pools within soils and sediments. Forest ecosystems, through organic matter decomposition and mineralization processes, contribute to phosphorus retention and gradual nutrient release within surface soils. phosphorus Across different land use and land cover (LULC) systems, P stocks are generally dominated by inorganic forms, which account for approximately 60–80% of total phosphorus (Sukitprapanon et al., 2021; Yang et al., 2021).

phosphorus The elevated HCl-extractable phosphorus concentrations observed at anthropogenic and waste dumping locations in the present study indicate enhanced accumulation of calcium-associated phosphorus in sediments affected by anthropogenic nutrient inputs and land-use disturbance. In contrast, comparatively lower concentrations at forest and outlet sites suggest reduced phosphorus enrichment under relatively undisturbed environmental conditions. Seasonal increases during July and September 2024 further indicate the influence of runoff-driven sediment transport and phosphorus deposition processes. Phosphorus fractionation analyses further demonstrate that Ca-P, bioavailable phosphorus (BAP), and pH are important indicators for distinguishing between bioavailable and organic phosphorus pools. The results for

ACCEPTED MANUSCRIPT

recalcitrant phosphorus (0.5 M NaOH–Pt) observed in this study previous studies showing that recalcitrant organic phosphorus act as a long term phosphorus reservoir. Recalcitrant organic P often acts as a sink for phosphorus, slowly releasing it into available pools over time. Several studies have highlighted the role of occluded phosphorus as a major source that slowly release phosphorus through mineralization processes, thereby contributing to bioavailable and moderately available phosphorus pools in topsoil (Tiecher et al., 2020).

The elevated 0.5 M NaOH–Pt concentrations observed at anthropogenic and waste dumping locations in the present study indicate enhanced phosphorus retention and accumulation in sediments affected by anthropogenic nutrient inputs and organic matter enrichment. In contrast, forest and outlet sites exhibited comparatively lower concentrations, reflecting reduced phosphorus loading and lower sediment contamination under relatively undisturbed conditions. Seasonal increases during July and September 2024 further suggest the influence of runoff-driven sediment transport and nutrient deposition processes. Phosphorus fractionation studies have also shown that Fe and Al bound phosphorus pools are strongly influenced by hydrological and biogeochemical processes. Similar findings were reported by Zhuo et al. (2023) who demonstrated that sediment phosphorus concentrations are significantly influenced by hydrological variability and anthropogenic nutrient inputs, including fertilizers, manure, and urban or industrial waste. Increased runoff and sediment mobilization during wetter periods can enhance phosphorus transport and accumulation within depositional zones, particularly in disturbed catchments. Similar results from alkaline soils in Iran indicate that calcium-associated, phosphorus is often a dominant fraction of total phosphorus but can become mobilized under certain environmental conditions, particularly through organic matter inputs and hydrological changes (Jalali & Sajadi Tabar, 2011). The elevated residual phosphorus concentrations observed at anthropogenic and waste dumping locations in the present study indicate substantial long-term phosphorus accumulation within sediments influenced by human activities and nutrient enrichment processes. In contrast, forest and outlet sites exhibited comparatively lower residual P concentrations, suggesting reduced phosphorus loading and lower sediment contamination under relatively stable environmental conditions. Seasonal increases during July and September 2024 further indicate the influence of hydrological transport and sediment deposition processes on phosphorus accumulation.

ACCEPTED MANUSCRIPT

Climate variability and land-use change are important factors regulating sediment yield and phosphorus distribution within catchment systems. Previous studies from Azad Jammu and Kashmir reported that changes in forest cover significantly influence sediment transport and nutrient dynamics, where increased forest density was associated with reduced sediment disturbance and improved vegetation cover (Ahmad et al., 2025). The comparatively lower residual phosphorus concentrations observed at forest locations in the present study may therefore reflect the stabilizing effects of vegetation cover and reduced erosion intensity.

Residual phosphorus is generally considered a relatively stable and plant-unavailable phosphorus fraction, commonly associated with clay minerals and occluded phosphorus compounds. Previous studies have reported that residual phosphorus can account for approximately 25–53% of total phosphorus in soils and sediments, depending on land-use and environmental conditions (Wang & John Morrison, 2014). Ferric iron-bound phosphorus and organic phosphorus fractions have also been identified as important components regulating phosphorus retention and long-term storage within suspended particulate matter and sediment systems.

Land-use conversion has further been shown to significantly alter total phosphorus distribution and sediment nutrient dynamics. Kim et al. (2023) reported that conversion of alpine forest to grassland reduced total phosphorus concentrations substantially, whereas forest soils generally maintained higher phosphorus retention than cropland or shrub land systems. The elevated residual phosphorus concentrations recorded at anthropogenic and waste dumping sites in the present study therefore likely reflect cumulative nutrient loading, land-use disturbance, and prolonged sediment phosphorus storage within impacted areas.

Overall, these findings suggest that land-use change, vegetation cover, and hydrological processes strongly influence the accumulation and long-term stabilization of residual phosphorus fractions within the Goi-Nala catchment sediments.

The significantly higher total phosphorus (TP) concentrations observed at anthropogenic and waste dumping locations in the present study indicate substantial phosphorus enrichment associated with land-use disturbance, nutrient loading, and sediment deposition processes. In contrast, forest and outlet locations exhibited comparatively lower TP concentrations, suggesting reduced external phosphorus inputs and lower sediment-associated nutrient accumulation under relatively undisturbed environmental conditions. Seasonal increases during July and September

ACCEPTED MANUSCRIPT

2024 further suggest the influence of runoff-driven sediment transport and phosphorus mobilization during wetter periods.

Previous studies have shown that sediment phosphorus fractions in aquatic systems are strongly influenced by hydrological conditions, sediment characteristics, and anthropogenic nutrient inputs. Yang et al. (2024) reported that sediment total phosphorus concentrations in freshwater systems can vary considerably depending on environmental conditions and land-use patterns, with organic phosphorus representing an important component of total sediment phosphorus pools. Similar phosphorus fractionation patterns have also been observed in reservoir and riverine sediments, where Fe/Al-bound and calcium-associated phosphorus fractions dominate overall phosphorus storage. Mass balance and sediment accumulation studies further demonstrate the important role of riverine transport in phosphorus enrichment and eutrophication processes. Di et al. (2015) reported substantial annual phosphorus fluxes into lake sediments, indicating that freshwater catchments act as major sources of sediment-associated phosphorus loading. The elevated TP concentrations observed at anthropogenic and waste dumping locations in the present study therefore likely reflect cumulative nutrient transport, sediment deposition, and long-term phosphorus accumulation within impacted areas.

Long-term field experiments have additionally shown that excessive fertilizer and slurry applications can significantly increase particulate phosphorus losses and sediment phosphorus enrichment, particularly under disturbed land management systems (Tiecher et al., 2020). Increased phosphorus mobilization through runoff and erosion processes may therefore contribute to the elevated TP concentrations observed at anthropogenic and waste dumping sites within the Goi-Nala catchment.

Overall, these findings suggest that anthropogenic activities, land-use disturbance, and hydrological transport processes strongly regulate sediment total phosphorus accumulation and may increase eutrophication risk within the Goi-Nala catchment.

The findings of this study have important implications for watershed management and eutrophication control. The identification of bioavailable phosphorus fractions and the application of the SERI index provide a useful approach for identifying areas that contribute disproportionately to internal phosphorus loading. Management strategies should therefore focus on reducing sediment transport from agricultural and disturbed lands through erosion control measures, improved land-use practices, and sustainable nutrient management. Continuous

ACCEPTED MANUSCRIPT

monitoring of sediment phosphorus fractions can also support early detection of eutrophication risk and assist decision-makers in protecting freshwater ecosystems within the catchment.

4.3 SERI

The sediment eutrophication risk index (SERI) results indicated that there were definite seasonal and spatial changes throughout the study area. The low SERI values in July 2024 imply the lack of nutrient loading in the early dry season and a steep rise in the values of L2 in December 2024 is a sign of localized nutrient enrichment and potential eutrophication due to low water exchange and accretion of organic matter. Similar seasonal patterns have been reported in other aquatic systems, where stagnant or low-flow conditions enhance nutrient retention and algal productivity (Van Meter et al., 2020). The elevated SERI values observed during June–August 2025 are likely associated with post-monsoon runoff and agricultural inputs, consistent with findings from tropical and subtropical regions where rainfall events intensify nutrient inflow (Wang et al., 2025). Spatially, the persistently high SERI at L2 indicates greater anthropogenic influence, probably from agricultural drainage or domestic wastewater, as also noted by (Buckerfield et al., 2020).

Overall, the present results are in line with previous studies showing that seasonal hydrology, nutrient loading, and land-use intensity are key drivers of eutrophication dynamics. The Sediment Eutrophication Risk Index (SERI) proposed in this study differs from conventional eutrophication indicators that primarily rely on nutrient concentrations in the water column or trophic state indices (Jarvie et al., 2006). Instead, SERI focuses on sediment-bound phosphorus fractions and their potential bioavailability, which are key drivers of internal phosphorus loading in aquatic systems. By integrating phosphorus fractions with different mobility and bioavailability characteristics, the index provides a more comprehensive assessment of the potential contribution of sediments to eutrophication processes. The spatial and temporal patterns of SERI values observed in this study were consistent with measured phosphorus dynamics and seasonal hydrological variations in the catchment. This agreement suggests that the index effectively reflects sediment-related nutrient risks and can serve as a useful tool for assessing eutrophication potential in similar riverine environments.

Compared with widely used eutrophication assessment approaches, such as the Carlson Trophic State Index (TSI) and the OECD trophic classification, which primarily assess trophic status using water-column variables including total phosphorus, chlorophyll-*a*, and water

ACCEPTED MANUSCRIPT

transparency, SERI explicitly incorporates sediment phosphorus fractionation and bioavailable phosphorus to evaluate internal phosphorus loading. These established approaches were selected as conceptual reference methods because they are among the most widely applied frameworks for eutrophication assessment. Although they effectively characterize trophic status, they provide limited information on sediment-derived phosphorus release, which can sustain eutrophication even after external nutrient inputs decline (Jarvie et al., 2006). Consequently, SERI complements these conventional approaches by providing additional insight into sediment-driven nutrient cycling and long-term eutrophication risk, particularly in monsoon-influenced river systems.

The proposed SERI framework performed well because it integrates sediment phosphorus fractions with bioavailable phosphorus, providing a more realistic assessment of internal phosphorus loading than total phosphorus alone. However, its performance may be reduced in systems where eutrophication is primarily controlled by external nutrient inputs, hydrodynamics, or biological processes that are not included in the index. Therefore, future studies should integrate these factors to improve the robustness and broader applicability of the SERI framework.

4.4 Correlation of sediment characteristics and different P-fractions

The correlation matrix illustrating the relationships among sediment texture, total organic carbon (TOC), total nitrogen (TN), and phosphorus (P) fractions of varying lability under different seasonal and pollution conditions is presented in Fig. 11. Strong positive correlations were observed between TOC and TN ($r = 0.96$), indicating the close association between organic matter accumulation and nitrogen dynamics within the catchment sediments. Total organic carbon also showed strong positive relationships with bioavailable and moderately labile phosphorus fractions, including resin-extractable P and NaOH-extractable P fractions, as well as with HCl-extractable P, residual P, and total phosphorus. Similarly, TN exhibited significant positive correlations with several phosphorus fractions, particularly resin-P, NaOH-extractable P, residual P, and total phosphorus, suggesting that nutrient accumulation and phosphorus mobility are strongly influenced by organic matter and nitrogen enrichment.

Among the phosphorus fractions, significant interrelationships were observed between NaOH-extractable phosphorus fractions and other major phosphorus pools, including $NaHCO_3$-extractable P, HCl-bound P, residual P, and total phosphorus fractions. These associations indicate strong coupling among bioavailable, moderately labile and stable phosphorus pools

ACCEPTED MANUSCRIPT

within the sediment system. The observed relationships suggest that organic matter content and fine sediment particles play an important role in phosphorus retention, transformation, and cycling across the catchment. Similar correlations among soil properties and phosphorus fractions have also been reported in previous land-use and soil quality studies (Azene et al., 2022), supporting the influence of land-use change, sediment characteristics, and nutrient enrichment on phosphorus dynamics in freshwater environments.

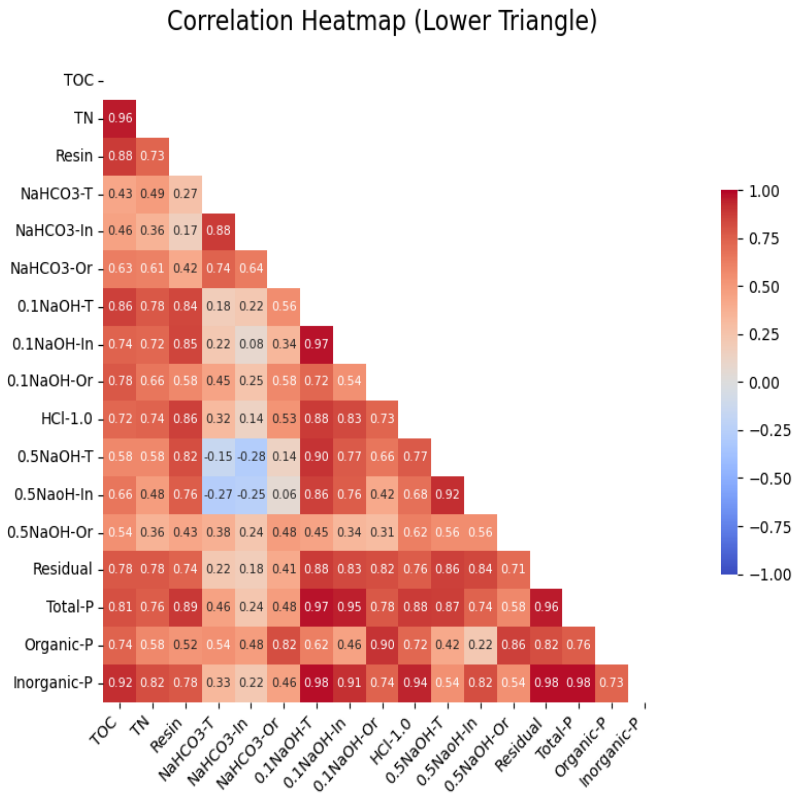


Fig. 11 Correlation coefficient among different sediment P-fractions, TOC and TN from the Goi-Nala catchment of River Jhelum, Azad Jammu and Kashmir (n = 18 ± 03).

The present study provides important insight into the spatial and temporal dynamics of sediment phosphorus fractions and their contribution to eutrophication risk within the Goi-Nala catchment. The consistently elevated phosphorus concentrations observed at anthropogenic and waste dumping locations demonstrate the strong influence of land-use disturbance and human activities on nutrient enrichment and sediment quality deterioration. The integration of phosphorus fractionation analysis with the Sediment Eutrophication Risk Index (SERI) offers a comprehensive approach for identifying eutrophication-sensitive zones and understanding

phosphorus mobility under varying environmental conditions. These findings highlight the importance of sediment-associated phosphorus as a potential long-term source of internal nutrient loading in freshwater ecosystems. Furthermore, the study provides baseline information that may support watershed management strategies, nutrient mitigation planning, and sustainable land-use practices aimed at reducing eutrophication risk and protecting water quality in Himalayan catchments and similar freshwater environments.

5. Conclusions and Future Perspective

This study evaluated the spatial and temporal variability of sediment phosphorus fractions and sediment eutrophication risk across contrasting land-use settings in the Goi-Nala Catchment, a monsoon-influenced Himalayan watershed. The results demonstrated significant spatial and seasonal variations in sediment phosphorus fractions ($p < 0.05$), reflecting the influence of land-use characteristics, anthropogenic pressures, and hydrological processes. Bioavailable phosphorus (anion exchange resin-extractable P) showed pronounced spatial variability, ranging from **4.46 mg kg^{-1}** at the forest site to **51.97 mg kg^{-1}** at the anthropogenic site, indicating greater phosphorus availability in areas influenced by human activities. Other phosphorus fractions, including $NaHCO_3$-extractable P, NaOH-extractable P, HCl-extractable P, residual phosphorus, and total phosphorus, also showed higher concentrations at impacted locations, particularly anthropogenic and waste-dumping sites, whereas forest sites generally exhibited lower phosphorus accumulation. Seasonal variations indicated enhanced phosphorus mobilization during monsoon and post-monsoon periods, likely associated with increased runoff, erosion, and sediment transport.

The proposed **Sediment Eutrophication Risk Index (SERI)** successfully differentiated spatial variations in sediment-associated eutrophication potential. The highest SERI value (**0.090**) was observed at the anthropogenic monitoring site (L2) during December 2024, corresponding with elevated bioavailable phosphorus concentrations. These findings indicate that anthropogenically influenced areas within the Goi-Nala catchment have greater susceptibility to sediment-mediated eutrophication processes. Elevated phosphorus accumulation at impacted sites was associated with urban influences, diffuse nutrient inputs, agricultural activities, and waste-disposal pressures. The integration of sequential phosphorus fractionation with the SERI framework provides a useful approach for assessing sediment phosphorus mobility and

ACCEPTED MANUSCRIPT

eutrophication risk in monsoon-driven river systems. This study establishes baseline information for identifying nutrient-sensitive areas and supports targeted monitoring and watershed management strategies aimed at reducing external phosphorus inputs and protecting freshwater ecosystems.

Future studies should evaluate the applicability of the SERI framework across additional river systems with varying climatic, geological, and land-use conditions. Long-term monitoring is recommended to assess changes in sediment phosphorus dynamics under future climatic and hydrological variability. Furthermore, combining sediment phosphorus fractionation with water-column nutrient measurements, biological indicators, and hydrological modeling would provide a more comprehensive understanding of phosphorus cycling and eutrophication processes. Assessment of management practices, including riparian restoration, erosion control, and improved nutrient management, may further support effective phosphorus reduction strategies in Himalayan and other monsoon-influenced freshwater systems.

5.1. Study Limitations

This study has several limitations that should be acknowledged. First, the investigation was conducted in a single monsoon-influenced catchment; therefore, the findings may not be directly transferable to watersheds with different climatic, geological, or land-use conditions. Second, although the monitoring period covered both wet and dry seasons, longer-term observations are needed to evaluate inter-annual variability in sediment phosphorus dynamics. Third, the proposed Sediment Eutrophication Risk Index (SERI) is based primarily on sediment phosphorus fractionation and bioavailable phosphorus and does not explicitly incorporate hydrodynamic processes, biological responses, or external nutrient inputs that may also influence eutrophication. In addition, the present assessment focused mainly on sediment phosphorus-related parameters; incorporating complementary environmental variables such as chlorophyll-*a*, dissolved oxygen, total nitrogen, oxidation–reduction potential, and hydrological characteristics would provide a more comprehensive evaluation of eutrophication processes. Finally, despite standardized sampling and laboratory quality-control procedures, natural spatial heterogeneity and seasonal fluctuations may introduce uncertainty into the measured phosphorus fractions. Therefore, the SERI framework should be considered a complementary assessment tool and

ACCEPTED MANUSCRIPT

should be further validated and refined using additional environmental parameters across diverse river systems and under different environmental conditions.

Declaration

All authors declare that there is no conflict of interest.

AI Statement

We used AI to improve the language.

Data Availability Statement

The data generated and analysed during the present study are available from the corresponding author upon reasonable request. The dataset includes the original measurements of sediment phosphorus fractions, bioavailable phosphorus, sediment physicochemical properties, and the calculated Sediment Eutrophication Risk Index (SERI) values supporting the findings of this study.

References

Ahmad, A., Ahmad, S. R., Gilani, H., & Nowosad, J. (2025). Assessment of forest fragmentation and ecological dynamics in Western Himalayan Region over three decades (1990–2020). *Environmental Monitoring and Assessment*, *197*(2), 205.

Ahmad, E. H., Ahmad, E. H., Demisie, W., & Zhang, M. (2017). Effects of Land Use on Concentrations and Chemical Forms of Phosphorus in Different-Size Aggregates. *Eurasian Soil Science*, *50*, 1435–1443.

Azene, B., Qiu, P., Zhu, R., Pan, K., Sun, X., Nigussie, Y., Yigez, B., Gruba, P., Wu, X., & Zhang, L. (2022). Response of soil phosphorus fractions to land use change in the subalpine ecosystems of Southeast margin of Qinghai-Tibet Plateau, Southwest China. *Ecological Indicators*, *144*, 109432.

Babur, M., Shrestha, S., Bhatta, B., Datta, A., & Ullah, H. (2020). Integrated assessment of extreme climate and landuse change impact on sediment yield in a mountainous transboundary watershed of India and Pakistan. *Journal of Mountain Science*, *17*(3), 624–640.

Bouyoucos, G. J. (1962). Hydrometer Method Improved for Making Particle Size Analyses of Soils1. *Agronomy Journal*, *54*, 464–465.

ACCEPTED MANUSCRIPT

739 Bremner, J. D., Campanella, C., Khan, Z., Shah, M., Hammadah, M., Wilmot, K., Al Mheid, I.,
740 Lima, B. B., Garcia, E. V., & Nye, J. (2018). Brain correlates of mental stress-induced
741 myocardial ischemia. *Biopsychosocial Science and Medicine*, *80*(6), 515–525.
742 Buckerfield, S. J., Quilliam, R. S., Bussiere, L., Waldron, S., Naylor, L. A., Li, S., & Oliver, D.
743 M. (2020). Chronic urban hotspots and agricultural drainage drive microbial pollution of
744 karst water resources in rural developing regions. *Science of the total environment*, *744*,
745 140898.
746 Centeri, C. (2022). Effects of grazing on water erosion, compaction and infiltration on
747 Grasslands. *Hydrology*, *9*(2), 34.
748 Chase, J. W., Benoy, G. A., & Culp, J. M. (2015). Combined effects of nutrient enrichment and
749 inorganic sedimentation on benthic biota in an experimental stream system. *Water*
750 *Quality Research Journal*, *52*(3), 151–165.
751 Condron, L. M., Goh, K. M., & Newman, R. H. (1985). Nature and distribution of soil
752 phosphorus as revealed by a sequential extraction method followed by 31P nuclear
753 magnetic resonance analysis. *European Journal of Soil Science*, *36*, 199–207.
754 Di, Z., Zhang, H., & Shan, B. (2015). Using sedimentary phosphorus/nitrogen as indicators of
755 shallow lake eutrophication: concentrations or accumulation fluxes. *Environmental Earth*
756 *Sciences*, *74*(5), 3935–3944.
757 Ellison, M. E., & Brett, M. T. (2006). Particulate phosphorus bioavailability as a function of
758 stream flow and land cover. *Water research*, *40*(6), 1258–1268.
759 Ferreira, T., Globevnik, L., & Schinegger, R. (2018). Water Stressors in Europe: New Threats in
760 the Old World. Multiple Stressors in River Ecosystems. Chapter. 8. In: Elsevier.
761 Gavrilaș, S., Burescu, F. L., Chereji, B. D., & Munteanu, F. D. (2025). The impact of
762 anthropogenic activities on the catchment's water quality parameters. *Water*, *17*(12),
763 1791.
764 Jalali, M., & Sajadi Tabar, S. (2011). Chemical fractionation of phosphorus in calcareous soils of
765 Hamedan, western Iran under different land use. *Journal of Plant Nutrition and Soil*
766 *Science*, *174*(4), 523–531.
767 Jarvie, H. P., Neal, C., & Withers, P. J. (2006). Sewage-effluent phosphorus: a greater risk to
768 river eutrophication than agricultural phosphorus?. *Science of the total*
769 *environment*, *360*(1-3), 246-253.

ACCEPTED MANUSCRIPT

Kianpoor Kalkhajeh, Y., Jabbarian Amiri, B., Huang, B., Henareh Khalyani, A., Hu, W., Gao, H., & Thompson, M. L. (2019). Methods for Sample Collection, Storage, and Analysis of Freshwater Phosphorus. *Water 11*(9), 1889.

Kim, D.-G., Kirschbaum, M. U., Eichler-Loebermann, B., Gifford, R. M., & Liáng, L. L. (2023). The effect of land-use change on soil C, N, P, and their stoichiometries: A global synthesis. *Agriculture, Ecosystems & Environment*, *348*, 108402.

Li, Q., Gray, K. E., & Jaisi, D. P. (2022). Relative Roles of Sediment Transport and Localized Erosion on Phosphorus Load in the Lower Susquehanna River and Its Mouth in the Chesapeake Bay, USA. *Journal of Geophysical Research: Biogeosciences, 127*(8).

Lizaga, I., Quijano, L., Gaspar, L., Ramos, M. C., & Navas, A. (2019). Linking land use changes to variation in soil properties in a Mediterranean mountain agroecosystem. *Catena*, *172*, 516–527.

Lv, Y., Zhang, M., & Yin, H. (2024). Phosphorus release from the sediment of a drinking water reservoir under the influence of seasonal hypoxia. *Science of the Total Environment*, *917*, 170490.

McDowell, R., Noble, A., Pletnyakov, P., & Mosley, L. (2021). Global Database of Diffuse Riverine Nitrogen and Phosphorus Loads and Yields, *Geoscience Data Journal, 8,* 132–143.

McDowell, R. W., Depree, C. V., & Stenger, R. (2020). Likely controls on dissolved reactive phosphorus concentrations in baseflow of an agricultural stream. *Journal of Soils and Sediments*, *20*, 3254 – 3265.

Muhammed, K. K., & Aziz, S. Q. (2025). Performance evaluation of recently constructed ponds for flood mitigation in Erbil City and their impacts on the environment. *Global Nest Journal*, *27*(7).

Maruthai, S., Rajendran, S., Selvanarayanan, R., & Gowri, S. (2025). Wastewater recycling integration with IoT sensor vision for real-time monitoring and transforming polluted ponds into clean ponds using HG-RNN. *Global Nest Journal*, *27*(4).

Murphy, J., & Riley, J. P. (1962). A modified single solution method for the determination of phosphate in natural waters. *Analytica chimica acta*, *27*, 31–36.

Nelson, D. W., & Sommers, L. E. (1983). Total Carbon, Organic Carbon, and Organic Matter. *SSSA Book Series*.

ACCEPTED MANUSCRIPT

Nweke, I., Nwosu, V., Okafor, J., & Maduke, C. (2025). Evaluation of structural stability, soil properties, quality and quantity of organic materials in soils of different history. *Discovery Agriculture,11.*

Phillips, J. M., Russell, M. A., & Walling, D. E. (2000). Time-integrated sampling of fluvial suspended sediment: A simple methodology for small catchments. *Hydrological Processes, 14*(14), 2589–2602. https://doi.org/10.1002/1099-1085(20001015)14:14

Pu, J., Ni, Z., & Wang, S. (2020). Characteristics of bioavailable phosphorus in sediment and potential environmental risks in Poyang Lake: the largest freshwater lake in China. *Ecological Indicators*, *115*, 106409.

Selvanarayanan, R., Rajendran, S., Pappa, C. K., & Thomas, B. (2024). Wastewater recycling to enhance environmental quality using fuzzy embedded with RNN-IOT for sustainable coffee farming. *Global Nest Journa, 26*(8). https://doi.org/10.30955/gnj.06346

Sharpley, A., Jarvie, H. P., Buda, A., May, L., Spears, B., & Kleinman, P. (2013). Phosphorus legacy: overcoming the effects of past management practices to mitigate future water quality impairment. *Journal of environmental quality*, *42*(5), 1308–1326.

Singh, S. K., & Rupp, H. (2026). Monitoring and modeling of runoff and soil processes in river basins. In (Vol. 14, pp. 1806978): Frontiers Media SA.

Sivasubramanian, S., Venkatesan, S. K. G., Thanarajan, T., & Rajendran, S. (2025). Al-Biruni Earth Radius Optimization for enhanced environmental data analysis in remote sensing imagery. *Agrociencia*, 1-18.

Sridhar, D. (2026). Rivers under stress: a comprehensive review on pollutant sources, human and ecological impacts, analytical, statistical, and geospatial methods and restoration strategies, for evaluating river water quality in India. *Environmental Geochemistry and Health*, *48*(4), 160.

Sukitprapanon, T. S., Jantamenchai, M., Tulaphitak, D., Prakongkep, N., Gilkes, R. J., & Vityakon, P. (2021). Influence of Application of Organic Residues of Different Biochemical Quality on Phosphorus Fractions in a Tropical Sandy Soil. *Agronomy*. *11*(2), 248.

Tiecher, T. L., Lourenzi, C. R., Girotto, E., Tiecher, T., Conti, L. D., Marques, A. C. R., Silva, L. O. S., Marchezan, C., Brunetto, G., & Ceretta, C. A. (2020). Phosphorus forms leached in

ACCEPTED MANUSCRIPT

a sandy Typic Hapludalf soil under no-tillage with successive pig slurry applications. *Agricultural Water Management*, *242*, 106406.

Tundu, C., Tumbare, M. J., & Kileshye Onema, J. M. (2018). Sedimentation and its impacts/effects on river system and reservoir water quality: case study of Mazowe catchment, Zimbabwe. *Proceedings of the International Association of Hydrological Sciences*, *377*, 57–66.

Van Meter, K. J., Chowdhury, S., Byrnes, D. K., & Basu, N. B. (2020). Biogeochemical asynchrony: Ecosystem drivers of seasonal concentration regimes across the Great Lakes Basin. *Limnology and Oceanography*, *65*(4), 848–862.

Vermeiren, C., Kerckhof, P., Reheul, D., & Smolders, E. (2022). Increasing soil organic carbon content can enhance the long-term availability of phosphorus in agricultural soils. *European Journal of Soil Science*, *73*(1), e13191.

Wang, C., & John Morrison, R. (2014). Phosphorus speciation and changes with depth in the sediment of Lake Illawarra, New South Wales, Australia. *Environmental Earth Sciences*, *71*(8), 3529–3541.

Wang, Y., Xu, H., Zhao, X., Kang, L., Qiu, Y., Paerl, H., Zhu, G., Li, H., Zhu, M., & Qin, B. (2025). Rainfall impacts on nonpoint nitrogen and phosphorus dynamics in an agricultural river in subtropical montane reservoir region of southeast China. *Journal of Environmental Sciences*, *149*, 551–563.

Xia, Y., Zhang, M., Tsang, D. C., Geng, N., Lu, D., Zhu, L., Igalavithana, A. D., Dissanayake, P. D., Rinklebe, J., & Yang, X. (2020). Recent advances in control technologies for non-point source pollution with nitrogen and phosphorous from agricultural runoff: current practices and future prospects. *Applied Biological Chemistry*, *63*(1), 8.

Yang, L. Y., Jiao, S. L., Wang, L., Li, Y. J., Yang, M., Feng, Y. L., Li, J., & Wei, Z. X. (2024). Characteristics and release risk of phosphorus from sediments in a Karst Canyon Reservoir, China. *Applied Sciences*, *14*(6), 2482.

Yang, L., Yang, Z., Zhong, X., Xu, C., Lin, Y., Fan, Y., Wang, M., Chen, G., & Yang, Y. (2021). Decreases in soil P availability are associated with soil organic P declines following forest conversion in subtropical China. *Catena*, *205*, 105459.

Zafar, M., Tiecher, T., de Castro Lima, J. A. M., Schaefer, G. L., Santanna, M. A., & Dos Santos, D. R. (2016). Phosphorus seasonal sorption-desorption kinetics in suspended

ACCEPTED MANUSCRIPT

sediment in response to land use and management in the Guaporé catchment, Southern Brazil. *Environmental monitoring and assessment*, *188*(11), 643.

Zalasiewicz, J., Williams, M., Haywood, A., & Ellis, M. (2011). The Anthropocene: a new epoch of geological time? *Philosophical Transactions of the Royal Society A: Mathematical, Physical and Engineering Sciences*, *369*(1938), 835–841.

Zhu, X., Liu, W., Chen, J., Bruijnzeel, L. A., Mao, Z., Yang, X., Cardinael, R., Meng, F. R., Sidle, R. C., & Seitz, S. (2020). Reductions in water, soil and nutrient losses and pesticide pollution in agroforestry practices: a review of evidence and processes. *Plant and Soil*, *453*(1), 45–86.

Zhuo, T., Wan, Q., Chai, B., Lei, X., He, L., & Chen, B. (2023). Microbial pathways in the coupling of iron, sulfur, and phosphorus cycles at the sediment–water interface of a river system: An in situ study involving the DGT technique. *Science of the Total Environment*, *863*, 160855.

ACCEPTED MANUSCRIPT